Experimental Characterization of Superradiance in a Single-Pass High-Gain Laser-Seeded Free-Electron Laser Amplifier

T. Watanabe,[1,*] X. J. Wang,[1] J. B. Murphy,[1] J. Rose,[1] Y. Shen,[1] T. Tsang,[2] L. Giannessi,[3] P. Musumeci,[4] and S. Reiche[5]

[1]*National Synchrotron Light Source, Brookhaven National Laboratory, Upton, New York 11973-5000, USA*

[2]*Instrumentation Division, Brookhaven National Laboratory, Upton, New York 11973-5000, USA*

[3]*ENEA C.R. Frascati, Via E. Fermi 45, 00044 Frascati, Italy*

[4]*INFN c/o Dipartimento di Fisica, Università di Roma "La Sapienza", Piazzale Aldo Moro 2, 00185 Roma, Italy*

[5]*Department of Physics and Astronomy, UCLA, Los Angeles, California 90095, USA*

(Received 15 September 2006; published 19 January 2007)

In this Letter we report the first experimental characterization of superradiance in a single-pass high-gain free-electron laser (FEL) seeded by a 150 femtosecond (FWHM) Ti:sapphire laser. The nonlinear energy gain after an exponential gain regime was observed. We also measured the evolution of the longitudinal phase space in both the exponential and superradiant regimes. The output FEL pulse duration was measured to be as short as 81 fs, a roughly 50% reduction compared to the input seed laser. The temporal distribution of the FEL radiation as predicted by a numerical simulation was experimentally verified for the first time.

DOI: 10.1103/PhysRevLett.98.034802 PACS numbers: 41.60.Cr, 42.25.Bs, 42.25.Kb

Three international laboratories are constructing single-pass high-gain free-electron lasers (FEL) to generate extremely bright coherent x-ray beams which will enable exciting new science in the fields of biology, chemistry, and physics [1]. For analysis of transient physical and chemical reactions on an atomic scale, one of the main requirements is to generate as short an FEL pulse as possible. The most straightforward approach to generate short FEL pulses would be to produce shorter e-beam bunches since all the FEL pulses generated by single-pass schemes to date have been determined by the electron beam bunch length [2–5]. However, high intensity short electron bunches are limited by peak current effects such as coherent synchrotron radiation (CSR) and longitudinal space charge effects.

Bonifacio and collaborators [6–12] have predicted a reduction of the light pulse length under certain conditions in an FEL. The term superradiance, originally coined by Dicke [13], was used to describe this pulse shortening regime in which the radiated FEL power is proportional to the square of the number of electrons in a cooperation length, $L_c = \lambda_r/4\pi\rho$ [14], where λ_r is the radiation wavelength and ρ is the Pierce parameter [15]. Some aspects of superradiance have been experimentally observed in FEL oscillators but until now superradiance has not been observed in an FEL amplifier [16,17]. Recently, Giannessi *et al.* proposed a novel scheme to generate femtosecond (fs) x-ray pulses based on a cascade of single-pass seeded FEL amplifiers operating in the superradiant regime [18].

In this Letter, we report the first experimental characterization of superradiance in a single-pass high-gain FEL seeded by a Ti:sapphire laser. The FEL output pulse length measured by a frequency-resolved optical gating (FROG) technique [19] was half that of the input seed laser and shorter than the electron beam by more than an order of magnitude. Simultaneously, we also observed the FEL spectral broadening in the superradiant regime by the FROG. The nonlinear gain of the FEL beyond the saturation of the exponential gain regime was also measured. Our experimental results are compared to both theoretical models and numerical simulations.

In the superradiant regime, the FEL pulse is compressed such that it can be significantly shorter than the input seed laser pulse. The pulse energy [E_{SR}], the pulse length [σ_{SR}] and the pulse peak power [P_{SR}] scale with the distance along the undulator [z] as follows [8,12,18],

$$E_{\mathrm{SR}} \propto z^{3/2}, \qquad \sigma_{\mathrm{SR}} \propto z^{-1/2}, \qquad P_{\mathrm{SR}} = \frac{E_{\mathrm{SR}}}{\sigma_{\mathrm{SR}}} \propto z^2. \quad (1)$$

Figure 1 depicts the evolution of the temporal and spectral distributions of the FEL light obtained by a numerical simulation with the GENESIS1.3 code [20] using the experimental parameters listed in Table I. The longitudinal profile of the radiation power and the spectrum are displayed along the undulator axis z in Figs. 1(a) and 1(b), respectively. In both figures, the profiles are normalized at each z. Since the simulation time window in Fig. 1(a) moves with the average velocity of the electrons [v_z], the slope of the FEL radiation power along the electron beam coordinate [$s \equiv t - z/v_z$] in Fig. 1(a) indicates the slippage of the radiation with respect to the electron pulse. In the simulation, the seed pulse is a Gaussian distribution with the duration of 150 fs of full width at half maximum (FWHM), and the electron pulse forms an asymmetric triangular distribution with 0.2 ps rise time and 1 ps decay at half maximum. Note that for the simulation we chose the same parameters as our experimental conditions so the peak current is not constant over the pulse.

In the superradiant regime the spectrum breaks into a wideband multipeak structure, with most of the energy

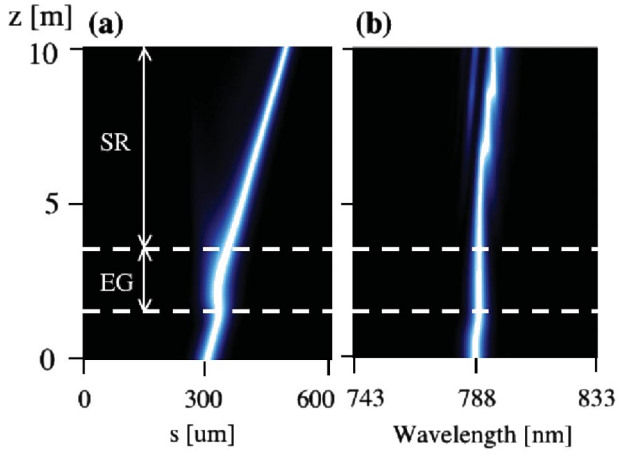

FIG. 1 (color). (a) Normalized longitudinal profile of the FEL radiation power along the electron beam coordinate "s" as it evolves along the undulator with coordinate "z" [18], and (b) spectral evolution along the undulator, as determined by a numerical simulation with GENESIS1.3 [20] using the experimental parameters in Table I. Note exponential gain (EG) regime and superradiant (SR) regime.

being redshifted [21]. It may be interpreted that as the superradiant pulse slips forward along the electron pulse, the radiation is emitted by fresh electrons that have no phase correlation with the radiation emitted behind.

For the FEL to reach the superradiant regime it must pass through the exponential gain regime (EG in Fig. 1). A laser-seeded FEL amplifier is a good platform to explore superradiance since the saturation of the exponential gain regime can be controlled by the seed laser intensity. In a laser-seeded FEL amplifier, the root-mean-squared (rms) pulse length and bandwidth of the FEL light evolve along the undulator length as [22],

$$\sigma_t(z) = \sigma_{t,s}\sqrt{1 + \frac{1 + 3\sigma_{t,s}^2\sigma_{\omega,\mathrm{GF}}^2(z)}{3\sigma_{t,s}^2\sigma_{\omega,\mathrm{GF}}^2(z)[1 + 4\sigma_{t,s}^2\sigma_{\omega,\mathrm{GF}}^2(z)]}}, \quad (2)$$

$$\sigma_\omega(z) = \frac{\sigma_{\omega,\mathrm{GF}}(z)}{\sqrt{1 + 4\sigma_{t,s}^2\sigma_{\omega,\mathrm{GF}}^2(z)}}, \quad (3)$$

TABLE I. Experimental parameters at the SDL.

Undulator period λ_u	3.89 cm
Undulator parameter K	1.1
Undulator length L_u	10 m
Electron energy E	102 MeV
Electron bunch length (FWHM)	1.2 ps
rms energy spread σ_E/E	0.1%
Maximum peak current I	400 A
Seed laser wavelength λ_s	788 nm
Seed laser bandwidth (FWHM) $\Delta\lambda_s$	6.7 nm
Seed laser duration (FWHM) τ_s	150 fs
Maximum peak power of seed laser	10 MW

where $\sigma_{t,s}$ is the seed laser pulse length and $\sigma_{\omega,\mathrm{GF}}(z) \equiv \sqrt{\frac{3\sqrt{3}\rho\omega_r^2}{k_u z}}$ is the FEL Green function bandwidth in the exponential gain regime, $k_u = 2\pi/\lambda_u$ and λ_u is the undulator period. The fact that the seed pulse is fully longitudinally coherent, $\sigma_{t,s}\sigma_{\omega,s} = 1/2$, has been used in the above formulas. From Eq. (2), it can be seen that the unchirped seed pulse can only stretch in the exponential gain regime, so any pulse shortening must occur in the superradiant regime. In addition, the bandwidth in the EG regime decreases monotonically along the undulator.

Another characteristic of the exponential gain regime is the reduction of the group velocity of the FEL pulse ($c \rightarrow v_g = \omega/(k + \frac{2}{3}k_u)$) which reduces the slippage of the FEL pulse relative to the electrons from the free space value [8,22]. One can clearly see this reduced slippage (increased slope) in the EG regime in Fig. 1.

The experiments reported here were performed at the Source Development Lab (SDL) of the Brookhaven National Laboratory (BNL). The SDL consists of an rf photoinjector, a 250 MeV linac, a 10-meter undulator, and a Ti:sapphire laser system. The single Ti:sapphire laser system with two separate optical compressors is used both to drive the rf gun and to seed the FEL. We have routinely conducted laser-seeded FEL amplifier experiments with the seed laser pulse length much longer than the electron beam, which produces saturated FEL pulses in which the FEL pulse duration is determined by the electron bunch length and the spectra are Gaussian [23]. To explore the superradiant regime, we use a similar setup, the key difference being that the optical compressor of the seed laser is adjusted so that the seed is nearly Fourier-transform-limited with an unchirped pulse duration of 150 fs and a bandwidth of 6.7 nm (FWHM) as shown in Fig. 3(e). The key experimental parameters are listed in Table I.

To maximize the effects of the superradiance, the seed laser energy is adjusted so that the FEL radiation in the exponential gain regime saturates at ~3.5 m into the 10 m undulator as shown in Fig. 1. In this case the FEL radiation grows very little in the exponential gain regime. To minimize the contamination of the FEL output measurement by the input seed laser, in Fig. 2 we begin the plot at $z \sim 5.8$ m where the FEL output is significantly stronger than the input seed. The timing jitter between the seed laser and the electron beam can result in the laser pulse arriving anywhere along the electron beam pulse, as such there is a large fluctuation in the sampled electron beam peak current which results in a large fluctuation of the FEL output. Thus, only the maximum radiation output is used in Fig. 2. One can see that the pulse energy continues to increase over the second half of the undulator in the superradiant regime. The energy gain of the superradiant pulse as given in Eq. (1) assumes a rectangular electron beam distribution, while in our experiment, the electron pulse distribution is better approximated by an asymmetric triangular distribution. In addition, the total energy measured

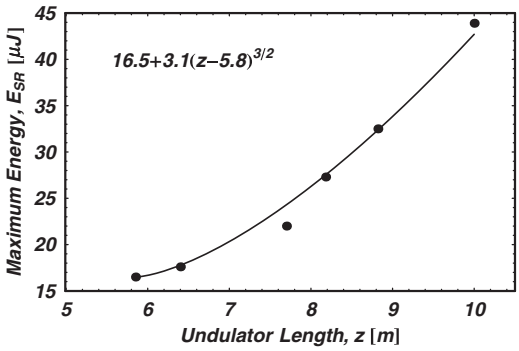

FIG. 2. Plot of the measured (dots) and fit (line) of the maximum pulse energy versus distance along the undulator in the superradiant regime.

in the experiment can also contain a contribution from self amplified spontaneous emission (SASE) emitted from electrons in the head and tail of the pulse. As a result, the measured energy gain curve scales close to, but not precisely, as $z^{3/2}$.

The longitudinal phase space distribution of the radiation was measured using a commercial Grenouille configuration FROG [19]. In the Grenouille setup, there is an intrinsic ambiguity in the direction of time in the temporal distributions which can be resolved by comparison with the numerical simulations.

Typical shots of the measured raw and retrieved FROG images of the FEL light are shown in the first two columns of Fig. 3, where the horizontal axis is the delay [τ] and the vertical axis is the frequency [ω]. The FROG images of the input seed laser is shown in the bottom row of Fig. 3. As expected the FROG images are very symmetric in time, and no significant difference between the raw and the retrieved images are found, which certifies the reliability of the data. The resulting temporal and spectral distributions, including the phase are also shown in columns 3 and 4 of Fig. 3 along with a label which highlights the duration of the main temporal peak (FWHM). The FROG images become increasingly complicated as the pulse duration is shortened. In the shortest case, the top row of Fig. 3, the image consists of multiple peaks in both time and spectrum.

Figure 4 redisplays the amplitude of temporal and spectral distributions for the measured FROG image (blue) shown in the first row of Fig. 3, together with the GENESIS1.3 simulation results (red). The arrow of time of the experimental results is set to match the simulation in which the secondary pulses are behind the main peak in time.

The pulse duration of the main peak in the experiment is 81.7 fs (FWHM), while that in the simulation is 86 fs, both are roughly half the seed pulse duration of 150 fs. In

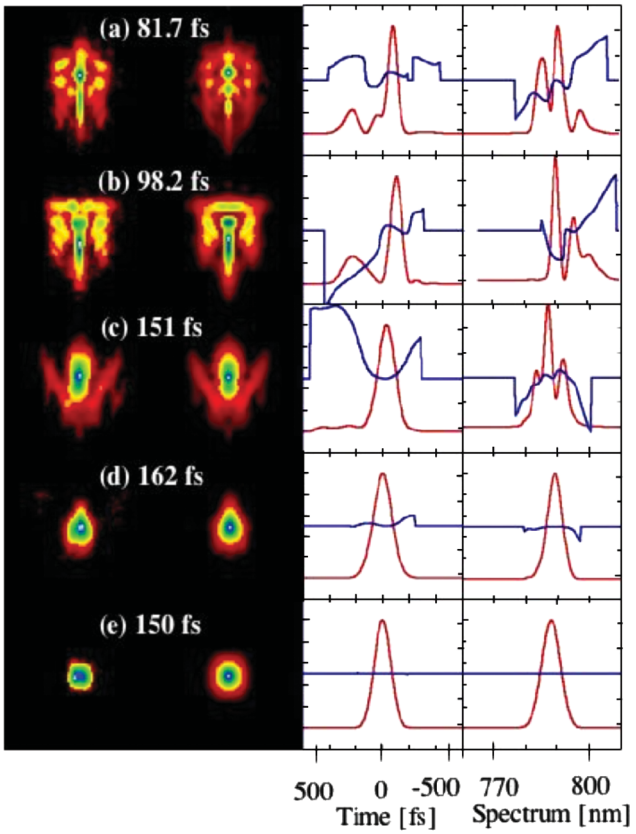

FIG. 3 (color). Each FROG result is a row in the figure labeled by the FWHM of the main temporal peak. Starting from the left, the four columns are: raw and retrieved FROG images, temporal and spectral distributions including phase. Amplitudes (red) are normalized and phase (blue) are plotted from −6 to +6 radians.

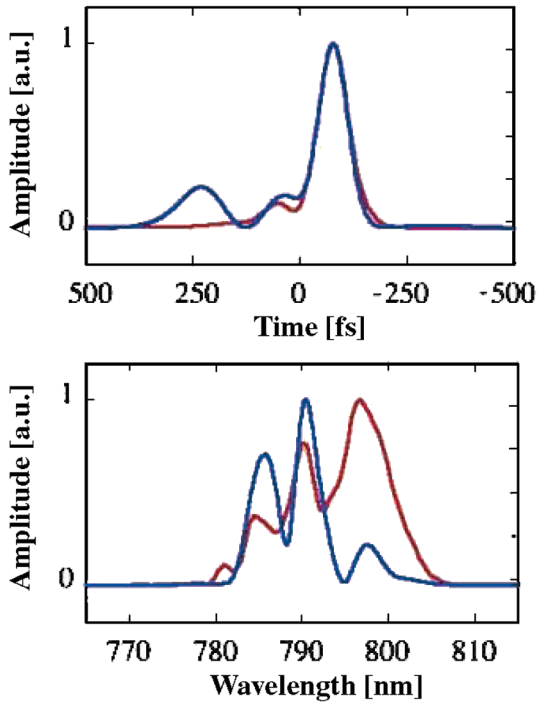

FIG. 4 (color). Measured FROG results of the first row of Fig. 3 (blue) and GENESIS1.3 simulation results (red). For the temporal distribution, toward the right is the head and left is the tail of the pulses.

addition to the main peak, secondary peaks are observed. Such a distribution has been observed in the earlier numerical analyses based on the superradiant theory [8,10,11,18]. Another notable feature is that in Fig. 3(a) the phase of the secondary peak is continuously shifted from the main peak, while there is a phase jump between the second and the third peaks. This indicates that the second pulse maintains a phase correlation with the main peak, while the third is independent from the first two peaks. Note that in the exponential gain regime, the longitudinal coherence of the seeded FEL is fully preserved, and the radiation pulse cannot be shorter than the seed laser when the input electron pulse is unchirped [see Eq. (2)] [22]. This further supports the fact that the pulse in Fig. 4 is superradiant, since the duration of the output FEL pulse is shorter than the seed laser and the longitudinal coherence in the output pulse has been deteriorated.

As shown in Figs. 1 and 4, the spectrum of the superradiant pulse becomes wider and spiky in both the simulation and experiment. Although the spectral width in the normal seeded FEL experiments with long pulse seeding was measured to be 10 nm peak to peak [23], both the numerical and experimental spectra in the superradiant regime spread out to 20 nm peak to peak and the centroid of the spectrum is redshifted [21].

Additionally, we shall discuss the observation of stretched pulses and the stability of our superradiance experiment. As shown in the third and fourth rows of Fig. 3, pulses longer than the seed laser were also measured. We attribute this to the shot-to-shot fluctuations in the electron bunch distribution and the timing jitter between the seed laser and the electron beam ($\sim$300 fs). The seed laser is occasionally launched at the edge of the electron bunch where the electron density is very low resulting in the saturation point being shifted far downstream in the undulator. In the fourth row of Fig. 3, the pulse durations is 161 fs (FWHM), which is longer than the seed laser, and the bandwidth is 5.5 nm (FWHM), which is narrower than the seed laser and the phase plots in the FROG images are smooth which implies that the coherence is preserved. These features are consistent with the Eqs. (2) and (3), indicating that this case did not make the transition past the exponential gain regime to superradiance [22]. In Fig. 3(c), the pulse duration is almost the same as the seed laser, while the spectrum is wide and consists of multiple peaks. The profiles have obviously evolved away from the seed laser in Fig. 3(e). In this case the pulse width will have grown in the exponential gain regime only to be reduced to approximately its initial value during the superradiant regime.

In conclusion, superradiance in a single-pass high-gain laser-seeded FEL was experimentally characterized for the first time. We observed the nonlinear energy gain after saturation of the exponential gain regime. The longitudinal pulse width evolution in both the exponential gain (pulse width grows) and superradiant regimes (pulse width shrinks) was measured. The measured spectral distribution agrees well with our numerical simulation. Note that the output pulse length was not determined by the electron bunch length, which is the first observation of this phenomena in a single-pass high-gain FEL. Our results may open a new avenue to realizing ultrashort pulses in an FEL.

The work of T. W., X. J. W., J. B. M., J. R., and Y. S. was supported by the U. S. Department of Energy under Contract No. DE-AC02-98CH10886 and the Office of Naval Research. The work of L. G. and P. M. has been partially supported by the EU Contract No. 011935 EUROFEL.

*Electronic address: twatanabe@bnl.gov

[1] J. Arthur *et al.*, SLAC Report No. SLAC-R-521, 1998; M. Altarelli *et al.*, DESY Report No. 2006-097, 2006; *"SCSS X-FEL Conceptual Design Report"*, SPRING8 Report, edited by T. Tanaka and T. Shintake, 2005.
[2] S. Milton *et al.*, Science **292**, 2037 (2001).
[3] V. Avyvazyah *et al.*, Phys. Rev. Lett. **88**, 104802 (2002).
[4] A. Tremaine *et al.*, Phys. Rev. Lett. **88**, 204801 (2002).
[5] L. H. Yu *et al.*, Phys. Rev. Lett. **91**, 074801 (2003).
[6] R. Bonifacio and F. Casagrande, Nucl. Instrum. Methods Phys. Res., Sect. A **239**, 36 (1985).
[7] R. Bonifacio *et al.*, Opt. Commun. **68**, 369 (1988).
[8] R. Bonifacio *et al.*, Nucl. Instrum. Methods Phys. Res., Sect. A **296**, 358 (1990).
[9] G. T. Moore and N. Piovella, IEEE J. Quantum Electron. **27**, 2522 (1991).
[10] N. Piovella, Opt. Commun. **83**, 92 (1991).
[11] R. Bonifacio, N. Piovella, and B. W. J. McNeil, Phys. Rev. A **44**, R3441 (1991).
[12] R. Bonifacio *et al.*, Phys. Rev. Lett. **73**, 70 (1994).
[13] R. H. Dicke, Phys. Rev. **93**, 99 (1954).
[14] J.-M. Wang and L.-H. Yu, Nucl. Instrum. Methods Phys. Res., Sect. A **250**, 484 (1986).
[15] R. Bonifacio, C. Pellegrini, and L. M. Narducci, Opt. Commun. **50**, 373 (1984).
[16] D. A. Jaroszynski *et al.*, Phys. Rev. Lett. **78**, 1699 (1997).
[17] R. Hajima and R. Nagai, Phys. Rev. Lett. **91**, 024801 (2003).
[18] L. Giannessi, P. Musumeci, and S. Spampinati, J. Appl. Phys. **98**, 043110 (2005).
[19] D. J. Kane and R. Trebino, IEEE J. Quantum Electron. **29**, 571 (1993).
[20] S. Reiche, Nucl. Instrum. Methods Phys. Res., Sect. A **429**, 243 (1999).
[21] W. Fawley, Proc. SPIE Int. Soc. Opt. Eng. **2988**, 98 (1997).
[22] J. B. Murphy, J. Wu, X. J. Wang, and T. Watanabe, BNL Report No. Report-75807-2006-JA, 2006.
[23] T. Watanabe *et al.*, *Proceedings of the 27th International Free Electron Laser Conference, 21-26 August 2005, Stanford, California*, JACoW/eConfC0508213 (2005), p. 98.